Journal for ImmunoTherapy of Cancer

Targeting CDCP1 boost CD8+ T cells-mediated cytotoxicity in cervical cancer via the JAK/STAT signaling pathway

Hua Huang ,[1,2] Yuwen Pan,[1,2] Qiuwen Mai,[1,2] Chunyu Zhang,[1,2] Qiqiao Du ,[1,2] Yuandong Liao,[1,2] Shuhang Qin,[1,2] Yili Chen,[1,2] Jiaming Huang,[1,2] Jie Li,[1,2] Tianyu Liu,[1,2] Qiaojian Zou,[1,2] Yijia Zhou,[1,2] Li Yuan,[1,2] Wei Wang,[1,2] Yanchun Liang,[1,2] Chao Yun Pan,[3] Junxiu Liu ,[1,2] Shuzhong Yao[1,2]

To cite: Huang H, Pan Y, Mai Q, *et al*. Targeting CDCP1 boost CD8+ T cells-mediated cytotoxicity in cervical cancer via the JAK/STAT signaling pathway. *Journal for ImmunoTherapy of Cancer* 2024;**12**:e009416. doi:10.1136/jitc-2024-009416

► Additional supplemental material is published online only. To view, please visit the journal online (https://doi.org/10.1136/jitc-2024-009416).

HH, YP and QM contributed equally.

Accepted 10 October 2024

[1]Department of Obstetrics and Gynecology, Sun Yat-sen University First Affiliated Hospital, Guangzhou, Guangdong, China
[2]Guangdong Provincial Clinical Research Center for Obstetrical and Gynecological Diseases, Guangzhou, Guangdong, China
[3]Department of Biochemistry, Sun Yat-Sen University, Guangzhou, Guangdong, China

Correspondence to
Dr Shuzhong Yao;
yaoshuzh@mail.sysu.edu.cn

Dr Junxiu Liu;
liujxiu@mail.sysu.edu.cn

ABSTRACT

Background Cervical cancer remains a global health challenge. The identification of new immunotherapeutic targets may provide a promising platform for advancing cervical cancer treatment.

Objective This study aims to investigate the role of CUB domain-containing protein 1 (CDCP1) in cervical cancer progression and evaluate its potential as a therapeutic target.

Methods We performed comprehensive analyses using patient cohorts and preclinical models to examine the association between CDCP1 expression and cervical cancer prognosis. Then in immunodeficient and immunocompetent mouse models, we further investigated the impact of CDCP1 on the tumor immune microenvironment, focusing on its effects on tumor-infiltrating T cells, including cytotoxic T lymphocytes (CTLs) and regulatory T cells (Tregs). Mechanistic studies were performed to elucidate the pathways involved in CDCP1-mediated immune modulation, in particular its interaction with the T cell receptor CD6 and the activation of the JAK-STAT signaling pathway.

Results Our results show that CDCP1 overexpression is associated with poor prognosis and T cell infliction in cervical cancer. Specifically, it affects the activity of CTLs and Tregs. Mechanistically, CDCP1 binds to CD6 and inhibits the JAK-STAT pathway of T cells. The study further demonstrates that targeting CDCP1 with the inhibitor 8-prenylnaringenin (8PN) effectively suppresses tumor growth in vivo and enhances antitumor immunity.

Conclusions CDCP1 plays a critical role in cervical cancer progression by modulating the tumor immune microenvironment. Targeting CDCP1 offers a promising therapeutic strategy to improve the outcome of patients with cervical cancer.

WHAT IS ALREADY KNOWN ON THIS TOPIC

⇒ CDCP1 is highly expressed in various malignant tumors and can directly influence tumor cell invasion and metastasis through signaling pathways such as PI3K/Akt, PKC5, SRC, and ERK/MAPK. However, its interaction with immune cells remains unexplored.

WHAT THIS STUDY ADDS

⇒ This study demonstrates that high expression of CDCP1 in cervical cancer can signals through CD6 on the surface of T cells, inhibit the JAK-STAT pathway within T cells, suppress the differentiation of cytotoxic T cells, promote the generation of Tregs, inhibit antitumor immunity, and facilitate the in vivo growth of cervical cancer tumors.

HOW THIS STUDY MIGHT AFFECT RESEARCH, PRACTICE OR POLICY

⇒ This study provides comprehensive experimental data supporting the potential of CDCP1 as a therapeutic target for immunotherapy in cervical cancer.

INTRODUCTION

Affecting women worldwide, cervical cancer ranks fourth in both incidence and mortality among gynecological tumors.[1 2] In 2022 alone, an estimated 604,000 new cases and 342,000 deaths were reported globally.[3] The standard of care for cervical cancer includes surgery, radiotherapy, and chemotherapy.[4 5] However, for patients with recurrent or metastatic cervical cancer, treatment with systemic therapy, unfortunately, results in a 5-year survival rate that remains below 20%.[6–10] Given the low cure rates of advanced-stage disease and the side effects of existing therapies, it is important to provide new treatment options for patients with cervical cancer. Immunotherapy, which aims to modify and harness the host immune system to more precisely and effectively target cancer cells, is emerging as a research hotspot and offers new hope for patients with cervical cancer. Checkpoint inhibitors targeting PD-1, PD-L1, and CTLA-4 have been extensively studied and have shown significant efficacy in certain cancer treatments.[11 12] However, response rates to pembrolizumab in cervical cancer remain relatively low at approximately 15%.[13] This emphasizes the need for a deeper understanding of the immune microenvironment

of cervical cancer and the identification of molecular targets with therapeutic potential.

Cervical cancer is driven by HPV infection, during which the virus evades immune surveillance and establishes an immunosuppressive environment by secreting cytokines, thereby reducing the recruitment of anti-inflammatory immune cells and inhibiting antitumor immunity.[14–16] Previous studies have suggested that the identification of potential immunotherapy targets should be based on three main criteria: targeting tumor-specific immune evasion mechanisms,[17 18] selective regulation of immunity within the tumor microenvironment,[19] and reprogramming antitumor immunity in the tumor microenvironment.[20 21] Increasing evidence suggests that impaired local immune function rather than systemic immune function plays an important role in the pathogenesis of cervical cancer.[22] Therefore, a thorough investigation of the immune microenvironment of cervical cancer is essential for the selection of potential immunotherapy targets. Li and Hua[23] conducted an analysis of the immune microenvironment in cervical cancer tissues using single-cell sequencing technology, which revealed a significant immunosuppressive state within the tumor characterized by abundant exhausted CD8+T cell infiltration. This finding is consistent with the sequencing results of Gu *et al* in the cervical cancer microenvironment,[24] as well as with studies on lung and liver cancer.[25 26] CD8+T cells, as key immune cells regulating the tumor microenvironment, are critical for antitumor immunity.[27] Effector T cells play an important role in the immune microenvironment of cervical cancer. Therefore, screening for molecules associated with T cell function holds promise as critical targets for reprogramming the cervical cancer immune microenvironment and enhancing antitumor immune responses.[12 28]

In 2001, Scherl-Mostageer *et al* first identified the overexpression of the CUB domain-containing protein 1 (CDCP1), a transmembrane protein also known as CD318, SIMA135, and TRASK, in colorectal cancer.[29] Over the past two decades, CDCP1 has been found to be highly expressed in various malignant tumors and closely associated with patient metastasis, recurrence, poor prognosis, and treatment response, including prostate cancer,[30 31] breast cancer,[32] lung cancer,[33 34] ovarian cancer,[35] bladder cancer,[36] and pancreatic cancer.[37–39] Further research has revealed the important role of CDCP1 in regulating molecular cascades reactions within tumor cells that are critical for tumor cell survival, growth, metastasis, and treatment resistance. For example, CDCP1 can interact with Src to reduce the adhesive phenotype of tumor cells and promote tumor metastasis.[40] In addition, CDCP1 can directly interact with EGFR or Her2, to enhance protumor signals, thereby promoting cancer cell dissemination or inducing drug resistance.[41] In Ras mutant tumors, CDCP1 is activated through the Ras/ERK signaling pathway, increasing MMP2 activation and MMP9 secretion, ultimately promoting tumor invasion and metastasis by degrading the extracellular matrix.[42] Although some evidence suggests the involvement of CDCP1 in cervical cancer progression,[43 44] the precise mechanistic role of CDCP1 in cervical cancer, particularly in the tumor microenvironment, remains to be elucidated. Therefore, elucidating the molecular mechanisms by which CDCP1 influences cervical cancer progression is of paramount importance for the development of novel therapeutic strategies to improve patient prognosis.

In this study, we aim to elucidate the role of CDCP1 in cervical cancer progression and explore its potential as a therapeutic target. We will examine the expression levels of CDCP1 in cervical cancer tissues and correlate them with clinical outcomes to assess their prognostic significance. In addition, we will use in vitro and in vivo models to determine the impact of CDCP1 on tumor growth and to investigate its influence on the tumor immune microenvironment, particularly its role in regulating tumor-infiltrating T cells. By exploring the biological functions, molecular mechanisms, and interactions with the immune system of CDCP1, we hope to provide novel targets and strategies for the treatment of cervical cancer.

MATERIALS AND METHODS

Clinical specimens

From January 2012 to December 2020, a total of 206 paraffin section specimens were collected from patients who underwent radical hysterectomy for cervical cancer. None of these patients had received radiotherapy or chemotherapy prior to surgery, and all had complete pathological information available. In addition, cervical tissue was collected from 30 patients who underwent hysterectomy for non-malignant conditions as controls.

TCGA data analysis

The TCGA database contains mRNA sequencing data from 306 cases of cervical cancer tissue. Normalization of gene expression values was performed, followed by the calculation of cytotoxic T lymphocyte (CTL) scores for each patient with cervical cancer.[45] CTL scores were determined by averaging the expression levels of CTL markers: CD8A, CD8B, GZMA, GZMB, and PRF1. Patients were classified into high and low CTL score groups based on whether their CTL score exceeded the average CTL score of all patients. EdgeR differential gene analysis was performed between the two groups, with a |log2FC| cut-off of 2 and a p value cut-off of 0.01. Overall survival and disease-free survival analyses were performed using the group median as the cut-off. TCGA heatmap visualizing CTL-associated gene and CDCP1 expression patterns in patients with cervical cancer using color gradients.

Cell culture

The human cervical cancer cell line SiHa and the mouse cervical cancer cell line U14 were both obtained from the Shanghai Institute of Life Sciences (Chinese Academy of Sciences). Human T cells were isolated from the peripheral blood of healthy volunteers, and mouse T cells were

isolated from the spleen of C57 mice. Cell culture media were as follows: For tumor cell culture, Dulbecco's modified Eagle's medium (Gibco) supplemented with 10% fetal bovine serum, L-glutamine, penicillin, and streptomycin. For T-cell culture, serum-free x-VIVO 15 medium supplemented with 200 U/mL of IL-2 was used. Cultures were maintained at 37°C in a humidified atmosphere containing 5% CO_2.

Cell transfection

U14 cells were transiently transfected with SiRNA(CRN1023, Cohexion) using Lipofectamine (Thermo Fisher, USA). U14/SiHa cells were transfected with ShRNA/plasmids targeting CDCP1 using lentiviral vectors. The designed targeting sequences for CDCP1 were as follows:
Murine-ShRNA-F: CCGGCCATCAAGTATGCAGTGAATTCTCGAGAATTCACTGCATACTTGATGGTTTTTG
Murine-ShRNA-R: AATTCAAAAACCATCAAGTATGCAGTGAATTCTCGAGAATTCACTGCATACTTGATGG
Human-ShRNA-F: CCGGCCTCAACTTCAATGTCTCCAACTCGAGTTGGAGACATTGAAGTTGAGGTTTTTG
Human-ShRNA-R: AATTCAAAAACCTCAACTTCAATGTCTCCAACTCGAGTTGGAGACATTGAAGTTGAGG.

The plasmids used included pLKO.1-Puro (P0258), pSIN-EF2-Puro (P40791), and pSIN-EF1a-Cdcp1 (mouse)-Puro (P50225), all purchased from MiaoLing Biology, China. Virus packaging and harvests were performed using 293 t cells. Fresh virus supernatant was collected for infection of U14/SiHa cells, followed by selection with 4/2 µg/mL puromycin (Beyotime) to obtain CDCP1 knockdown cells, CDCP1 overexpressing cells, and their respective control cells.

RNA Isolation and qPCR

After cell precipitation and washing, cellular RNA was extracted using the RNA-Quick Purification Kit (RN001, ES Science) according to the manufacturer's instructions. Total RNA concentration was measured using the NanoDrop2000, and cDNA synthesis was performed using the Reverse Transcription Kit (R223-01, Vazyme) according to the manufacturer's protocol. Subsequently, RT-qPCR was then performed using the qPCR reagent kit (AG11701, Accurate Biology) with the appropriate reaction setup. The following primer sequences were used:
Human-CDCP1-F: CTGAACTGCGGGGTCTCTATC.
Human-CDCP1-R: GTCCCCAGCTTTATGAGAACTG
Murine-CDCP1-F: GAGCTACCCATCCTCAACAGA.
Murine-CDCP1-R: GTCGAGGGGTTGCGAACTG.
Murine-IFN-γ-F: CAGCAACAGCAAGGCGAAAAAGG.
Murine-IFN-γ-R: TTTCCGCTTCCTGAGGCTGGAT.
Murine-IFNγR1-F: CTTGAACCCTGTCGTATGCTGG.
Murine-IFNγR1 -R: TTGGTGCAGGAATCAGTCCAGG
Murine-IL2-F: GCGGCATGTTCTGGATTTGACTC.
Murine-IL2-R: CCACCACAGTTGCTGACTCATC.
Murine-IL6-F: TACCACTTCACAAGTCGGAGGC.
Murine-IL6-R: CTGCAAGTGCATCATCGTTGTTC.
Murine-IL10-F: CGGGAAGACAATAACTGCACCC.
Murine-IL10-R: CGGTTAGCAGTATGTTGTCCAGC.
Murine-ACTB-F: GTGACGTTGACATCCGTAAAGA.
Murine-ACTB-R: GCCGGACTCATCGTACTCC.
Human-ACTB-F: CATGTACGTTGCTATCCAGGC.
Human -ACTB-R: CTCCTTAATGTCACGCACGAT.

Immunoprecipitation

Cell lysates were incubated with 4 µg of precipitating anti-CD6 antibody for 1 hour at room temperature. Then 50 µL of Protein A-Agarose solution was added and the mixture was incubated for 1 hour at room temperature. Finally, the samples were resuspended in 20 µL elution buffer for subsequent immunoblotting.

Western blot

Cell lysates were harvested and cells were lysed in 1×SDS sample buffer (Beyotime), resolved by 10% SDS-PAGE, and then transferred to a 0.45 µm PVDF membrane. The membrane was blocked with 5% skim milk in PBST for 60 min at room temperature. The primary antibodies were then incubated overnight at 4°C. The antibodies used were as follows: anti-CDCP1 antibodies (ab1377, Abcam and YT5291, Immunoway), anti-JAK1 antibody (#3332S, CST), Phospho-Jak1 (Tyr1034/1035) antibody (#3331, CST), anti-STAT1 antibody (AF6300, Affinity), Phospho-STAT1 (Tyr701) antibody (AF3300, Affinity), anti-STAT3 antibody (AF6294, Affinity), Phospho-STAT3 (Tyr705) antibody (AF3293, Affinity), and Beta Actin Monoclonal antibody (66009-1, Proteintech). After washing the bands, secondary antibodies were added and incubated for 1 hour at room temperature, followed by detection using enhanced chemiluminescence detection. The band intensities were quantified using ImageJ software.

Immunohistochemistry

Five µm paraffin sections were deparaffinized in fresh xylene, hydrated in a gradient of ethanol, subjected to high temperature high pressure antigen retrieval with alkaline EDTA, and blocked with goat serum. Antibodies (anti-CDCP1 antibody (ab1377, Abcam), anti-CD8 antibody (ZA-0508, ZSGB-BIO), anti-CD3 antibody (ZA-0503, ZSGB-BIO)) were then incubated overnight at 4°C. After the slides were washed, HRP-conjugated secondary antibodies were applied and incubated for 1 hour at room temperature. DAB staining was performed, followed by counterstaining with hematoxylin, dehydration through an ethanol gradient, and mounting in neutral resin. Immunohistochemical scoring was conducted based on the product of staining area and intensity (staining area score: 0=0%, 1=<25%, 2=25%–50%, 3=50%–75%, 4=>75%; staining intensity score: 0=no staining, 1=weak staining, 2=moderate staining, 3=strong staining), with scores by two experienced pathologists. Patients were divided into high-staining and low-staining groups based on a median score of 6.

Immunofluorescence

Five µm paraffin-embedded tissue sections were deparaffinized in xylene and rehydrated through an ethanol

gradient. Antigen retrieval was performed using alkaline EDTA at high temperatures. Sections were then blocked with 5% bovine serum albumin (BSA) and incubated with primary antibodies (anti-CDCP1, anti-CD8) overnight at 4°C. After washing with PBS, sections were incubated with fluorophore-conjugated secondary antibodies (AF488 and AF555, Thermo) for 1 hour at room temperature in the dark. Nuclei were stained with 4',6-diamidino-2-phenylindole (DAPI), and sections were mounted using anti-fade medium. Fluorescence microscopy was used for imaging, and the staining intensity was evaluated based on the fluorescence signal.

Immunofluorescence labeling

The SiHa human cervical cancer cell line was cultured at appropriate density in confocal dishes. The cells were then incubated with 1 µg/mL recombinant human CD6-Fc fusion protein(17051-H02H-100, Sino Biological) or human IgG-Fc fusion protein (fusion protein, Sino Biological) at 37°C for 4 hours according to the experimental design.[46] After incubation, cell monolayers were fixed and permeabilized with 100% methanol for 15 min at −20°C. After blocking with 1×PBS containing 10% normal donkey serum, 0.3% Triton X-100, and 1% BSA for 1 hour, the cells were incubated with primary antibodies (anti-CDCP1, Alexa Fluor 488 donkey anti-human IgG (K0001D-AF488, Solarbio)) overnight at 4°C. After washing, the cells were incubated with secondary antibodies (Alexa Fluor 555 donkey anti-rabbit) for 2 hours. After washing, the nuclei were stained with DAPI. The stained cells were then observed and recorded using an inverted fluorescence microscope (LSM780, Zeiss).

Cell proliferation assay

Transiently transfected CDCP1 knockdown or overexpressing U14 cells and their control groups were seeded at a concentration of 5000 cells per well in a 96-well plate and incubated at 37°C with 5% CO_2. CCK-8 viability assay (GK10001, GLPBIO) was performed every 24 hours for five consecutive days. Stable transfectants of CDCP1 knockdown or overexpressing U14 cells after lentiviral infection, together with their control groups, were seeded at a concentration of 2000 cells per well in a 6-well plate and incubated at 37°C with 5% CO_2. After 14 days, cells were fixed with 4% paraformaldehyde and stained with crystal violet. Cell clone formation was quantified using ImageJ.

In vitro co-culture experiment

T cells were isolated from C57 mouse spleen and human peripheral blood mononuclear cells (PBMCs) by magnetic bead separation according to the manufacturer's instructions (EasySep Mouse Pan-Naïve T Cell Isolation Kit, 19848, STEMCELL Technologies; EasySep Direct Human T Cell Isolation Kit, 720305, 19661, STEMCELL Technologies). The isolated mouse-derived and human-derived T cells were then separately co-cultured with CDCP1 knockdown or overexpressing U14 and SiHa cells, along with their corresponding control cells, at a ratio of 10:1. Part of T cells in certain experimental groups were preincubated with 10 µg/mL anti-CD6(MAB7271,R&D SYSTEMS) or IgG (BN20604, BIORIGIN) or 12.5 µM 8PN (I332693, Aladdin for 6 hours before co-culture).[47 48] Part of the co-culture systems was supplemented with anti-CD3/CD28 (Anti-Mouse CD28 SAFIRE Purified, 10312-25-500, PeproTech; Anti-Mouse CD3 SAFIRE Purified, 05112-25-500, PeproTech; ImmunoCult Human CD3/CD28 T Cell Activator, 10971, STEMCELL Technologies) for activation based on the experimental group. Subsequently, tumor cell-specific killing was evaluated by crystal violet staining, and T cell functional changes were analyzed by flow cytometry and Western blotting. In addition, in some of the co-culture systems, T cells were sorted via flow cytometry and subjected to downstream RNA sequencing to further investigate the molecular changes associated with the co-culture conditions.

Flow cytometry

All fluorescent antibodies used for flow cytometry were purchased from Biolegend. For human samples, fluorescent-conjugated antibodies included PerCP/Cy5.5 anti-human CD3, FITC anti-human CD4, Pacific Blue anti-human CD8, antigen-presenting cell (APC) anti-human CD137, and PE anti-human CD107a. For mouse samples, fluorescent-conjugated antibodies included APC/FIRE750 anti-mouse CD45.2, Percp5.5 anti-mouse F4/80, APC anti-mouse CD11b, BV650 anti-mouse CD11C, FITC anti-mouse GR1, BV421 anti-mouse ly6G, PE anti-mouse ly6C, FITC anti-mouse CD3, AF700 anti-mouse CD4, BV650 anti-mouse CD8, PE anti-mouse CD25, AF647 anti-mouse Foxp3, BV605 anti-mouse IFNγ, and PC7 anti-mouse GZMB. Subcutaneous tumors were digested into single-cell suspensions. Single cell suspensions were washed and then blocked with Mouse BD Fc Block at 4°C. Single cell suspensions were stained with a viability dye (Zombie Aqua Fixable Viability Kit, Biolegend) to exclude dead cells. Surface immunofluorescense staining was performed at 4°C for 30 min. For intracellular cytokine staining, cells were stimulated with 50 ng/mL PMA (P8139, Sigma-Aldrich) and 500 ng/mL ionomycin (Sigma-Aldrich) in the presence of brefeldin A (BD Bioscience) for 4 hours. After stimulation, cells were surface stained, fixed, and permeabilized with Biolegend Fixation/Permeabilization Buffer, followed by antibody staining at 4°C for 50 min. After washing, samples were analyzed using the Cytek Aurora flow cytometer, and the fluorescence data were analyzed using flowJo software.

Flow cytometry sorting

Following viability staining, the cells were further labeled with APC anti-mouse CD3. APC-positive ($CD3^+$) and Zombie-Aqua-negative (live) T cells were then sorted using a FACSAria cell sorter (BD Biosciences). The sorted live $CD3^+$ T cells were collected directly into RNAase-free tubes for subsequent RNA sequencing and other downstream applications.

Animal experiments

The animal experiments in this study were conducted under the approval of the Animal Ethics and Welfare Committee of Sun Yat-sen University. SPF-grade BALB/c nude mice (4–6 weeks old, 18–20 g, female) and C57BL/6 mice (4–6 weeks old, 18–20 g, female) were purchased from the Guangdong Medical Laboratory Animal Center and housed under SPF conditions throughout the experiments. For xenograft tumor formation, 100 µL containing 110^6 U14 cells (including CDCP1 knockdown or overexpressing U14 cells and their control groups) were injected subcutaneously into the mice. Tumor length (L) and width (W) were measured every other day using calipers, and tumor volume was calculated using the formula $V=L\times W^2/2$. For in vivo treatment, when the subcutaneous tumors reached approximately 100 mm^3 (around day 10), mice were randomly divided into groups and treated with injections of 10 mg/kg of anti-PD-1 antibody (BE0146, BioXcell), anti-CD6, isotype IgG control (BE0083, BioXcell), or 8PN.[47 48] three times a week according to the experimental design.[49] Human endpoints were achieved when tumor burden exceeded 1500 mm^3 or after 30 days.

Statistical analysis

Statistical analysis was performed by using Prism V.9 (GraphPad Software). The relationship between CDCP1 expression and clinicopathologic features was analyzed using the χ^2 test and Fisher's exact test. Survival analysis was performed using the Kaplan-Meier method and log-rank test. Data are presented as mean±SEM and evaluated by two-tailed Student's t-test. A value of $p<0.05$ was considered statistically significant.

RESULT

Identified CDCP1 correlated with poor prognosis and involved in regulating CTL function in cervical cancer

First, we evaluated the CTL scores based on the expression levels of CD8A, CD8B, GZMA, GZMB, and PRF1 in the TCGA-CESC(The Cancer Genome Atlas-Cervical squamous cell carcinoma and endocervical adenocarcinoma) cohort.[45] The overall survival analysis revealed that patients with high CTL scores had a significantly better prognosis compared with those with low CTL scores (figure 1A). Based on the methods of Chen Leping's team,[50] we explored potential targets for immunotherapy by identifying membrane proteins associated with immune infiltration within tumors. Therefore, we performed differential gene analysis on these two patient groups. Subsequently, differential expression analysis identified five membrane proteins potentially involved in regulating CTL function in cervical cancer, including ITGAL, PTPRC, PTPRN, WAS, and CDCP1 (figure 1B). Furthermore, we performed survival analysis on these five membrane proteins and found that only the expression level of CDCP1 was associated with patient prognosis (online supplemental figure S1A). Therefore, by survival analysis and differential gene analysis based on immune scores from the TCGA cervical cancer database, we identified CDCP1, a membrane protein-coding gene (figure 1C), which is associated with patient prognosis. CDCP1 is highly expressed in the low CTL scoring group and may play a role in regulating CTL function in cervical cancer.

To further investigate the role of CDCP1 in cervical cancer, we examined its expression levels in a cohort of patients from the First Affiliated Hospital, Sun Yat-sen University. Both mRNA and protein expression levels of CDCP1 were significantly increased in cervical cancer tissues compared with normal cervical samples (figure 1D,E). These findings suggest that CDCP1 overexpression is a common feature in cervical cancer and may serve as a prognostic biomarker for poor patient outcomes. Representative immunohistochemical images showed increased CDCP1 staining intensity in cervical cancer tissues compared with normal cervical tissues (figure 1F). The percentage analysis of low and high CDCP1 expression groups further confirmed the upregulation of CDCP1 in cervical cancer specimens (figure 1G). In addition, we performed an immunohistochemical analysis of tissue-infiltrating CD3+ and CD8+ T cells in 153 cases of cervical cancer tissues, comparing the CDCP1 high expression group with the CDCP1 low expression group (figure 1H). There was no association between the level of tissue infiltrating CD3+T cells and the level of CDCP1 expression in patients (figure 1H LEFT). However, tissues with high CDCP1 expression showed reduced infiltration of CD8+T cells (figure 1H RIGHT). Similarly, the expression level of CDCP1 is negatively correlated with functional markers of CTLs in the TCGA cervical cancer database (online supplemental figure S1B). We further analyzed the relationship between CDCP1 and pathological parameters related to the prognosis of cervical cancer in 176 patients (table 1). The expression level of CDCP1 is correlated with prognostic factors such as tumor size and pelvic lymph node metastasis, which affect the prognosis of cervical cancer. Importantly, overall survival analysis based on CDCP1 expression levels revealed a significant association between high CDCP1 expression and worse patient prognosis (figure 1I). Taken together, these results highlight the prognostic value of CDCP1 in cervical cancer and show its potential as a therapeutic target for further investigation.

The expression level of CDCP1 effected xenograft tumor growth in an immune-dependent manner

To investigate the role of CDCP1 in tumor growth, we used U14 cells with either CDCP1 knockdown or overexpression in mouse models. First, we subcutaneously injected control cells, CDCP1 knockdown, and overexpression U14 cells into 5-week-old female BALB/c-nu immunodeficient mice and 6-week-old female C57BL/6J immunocompetent mice (n=4 for each group). Representative images of tumor formation are shown in figure 2A,C. The tumor growth curve showed that CDCP1 knockdown significantly inhibited tumor growth

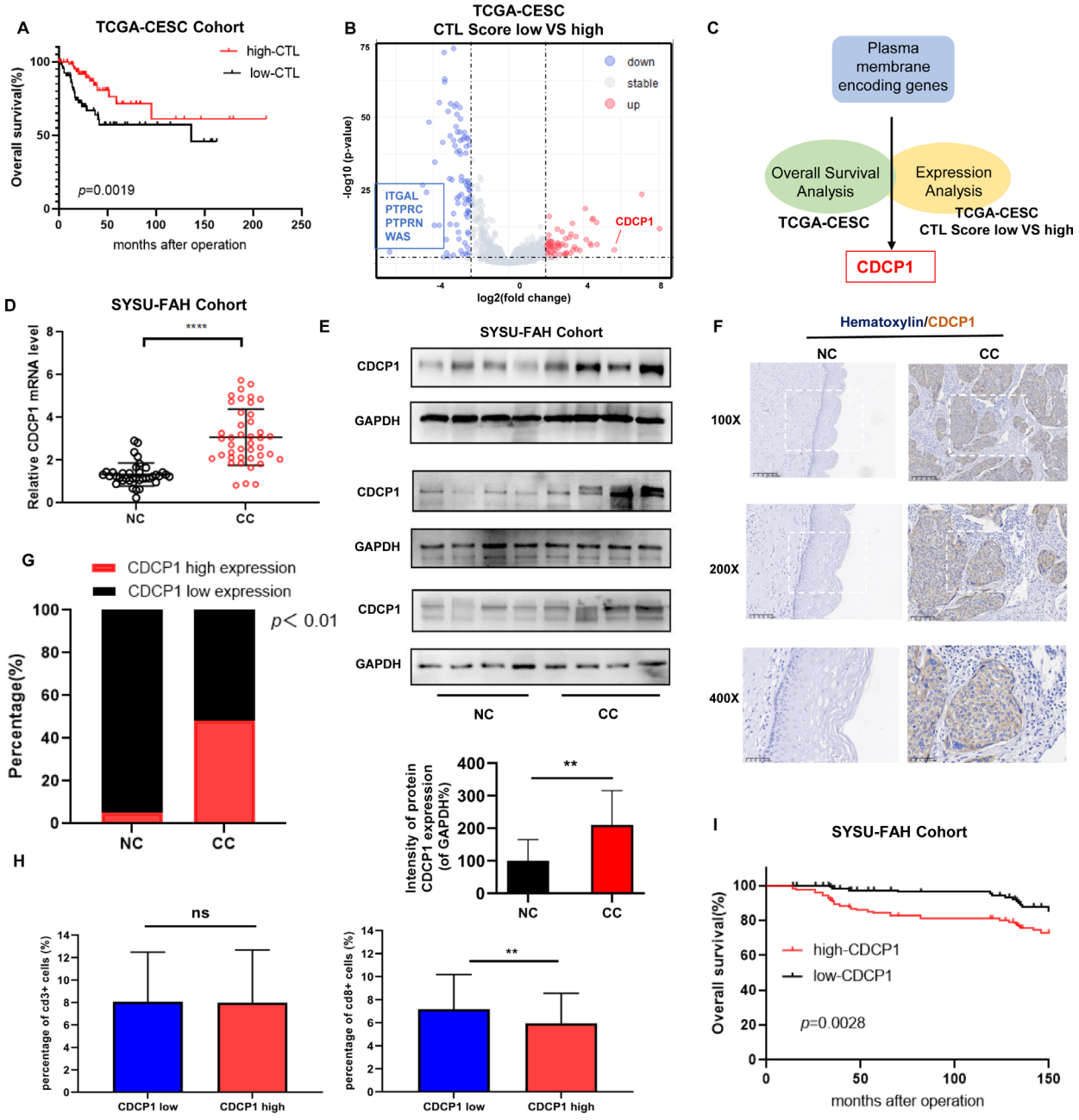

Figure 1 Identified CDCP1 correlated with poor prognosis and involved in regulating CTL function in cervical cancer. (A) Kaplan-Meier survival curves showing the overall survival of patients based on CTL scores (average expression of CD8A, CD8B, GZMA, GZMB, and PRF1) in TCGA-CESC(The Cancer Genome Atlas-Cervical squamous cell carcinoma and endocervical adenocarcinoma) Cohort. The log-rank test was used to determine the statistical significance of the difference between CDCP1 high/low expression groups, with p<0.05 considered statistically significant. (B) Volcano plot depicting the analysis of differentially expressed proteins between the CTL low-score group and the CTL high-score group. Each point corresponds to a gene, with genes exhibiting significant differential expression highlighted in red (upregulated in the CTL low-score group) and blue (downregulated in the CTL low-score group). Genes with |log2FC| greater than 2 and p<0.01 are considered significantly differentially expressed. Genes encoding membrane proteins that show significant differential expression are specifically labeled, including ITGAL, PTPRC, PTPRN, WAS, and CDCP1. (C) Schematic representation of systematic screening for immunotherapy targets in cervical cancer using the TCGA database. Through survival analysis and differential gene analysis based on immune scores from the TCGA cervical cancer dataset, membrane protein-coding genes associated with patient prognosis and low CTL scores were identified as potential targets for immunotherapy. (D) qRT-PCR analysis of CDCP1 mRNA expression levels in various patients sample.(E) Western blot analysis of NC (n=12) and CC (n=12) tissue samples. (F) Representative IHC images of CDCP1 staining in the NC and CC tissue samples. Bar in ×100, ×200, ×400 magnifications=200 µm, 100 µm, 50 µm, respectively. (G) Quantification of low and high CDCP1 expression percentages in the NC (n=30) and CC (n=176) groups based on the IHC staining results. Data are mean±SEM. Significance was determined using Student's t-test, "ns": not significant, **p<0.01, ****p<0.0001. CC, cervical cancer (n=56); CTL, cytotoxic T lymphocyte; IHC, immunohistochemistry; NC, normal cervix (n=35).

Table 1 The clinical and pathological parameters analysis of CDCP1 in cervical cancer

Clinicopathological variable	Total (N=176)	Low expression	High expression	P value
Age/years		92	84	
≤42	67	33	34	
>42	109	59	50	0.5296
FIGO stage				
Ia2	5	3	2	
Ib1	40	24	16	
Ib2	53	31	22	
Ib3	17	7	10	
IIa1	17	11	6	
IIa2	7	4	3	
IIB	3	2	1	
IIIC	34	10	24	0.1083
Tumor size				
≤4	135	77	58	
>4	41	15	26	**0.02166**
Pathological types				
Squamous cell carcinoma	152	79	73	
Adenocarcinoma	16	9	7	
Adenosquamous carcinoma	8	4	4	0.9438
Stromal invasion				
<1/2	68	33	35	
≥1/2	108	59	49	0.4302
Lymphovascular space invasion				
Yes	24	13	11	
No	152	79	73	0.8416
Differentiation grade				
Well	16	10	6	
Moderate	41	20	21	
Poor	119	62	57	0.6464
Pelvic lymph node metastasis				
Yes	34	10	24	
No	142	82	60	**0.002967**
Vaginal invasion				
Yes	27	17	10	
No	149	75	74	0.2268
Parametrial infiltration				
Yes	3	2	1	
No	173	90	83	1
Reccurrence				
Yes	14	2	12	
No	162	90	72	**0.003017**
Vital status at follow-up				
Alive	160	88	72	
Dead	16	4	12	**0.02198**

Significance was determined using Chi-squared test. Bold text indicates P< 0.05 and results are statistically significant.

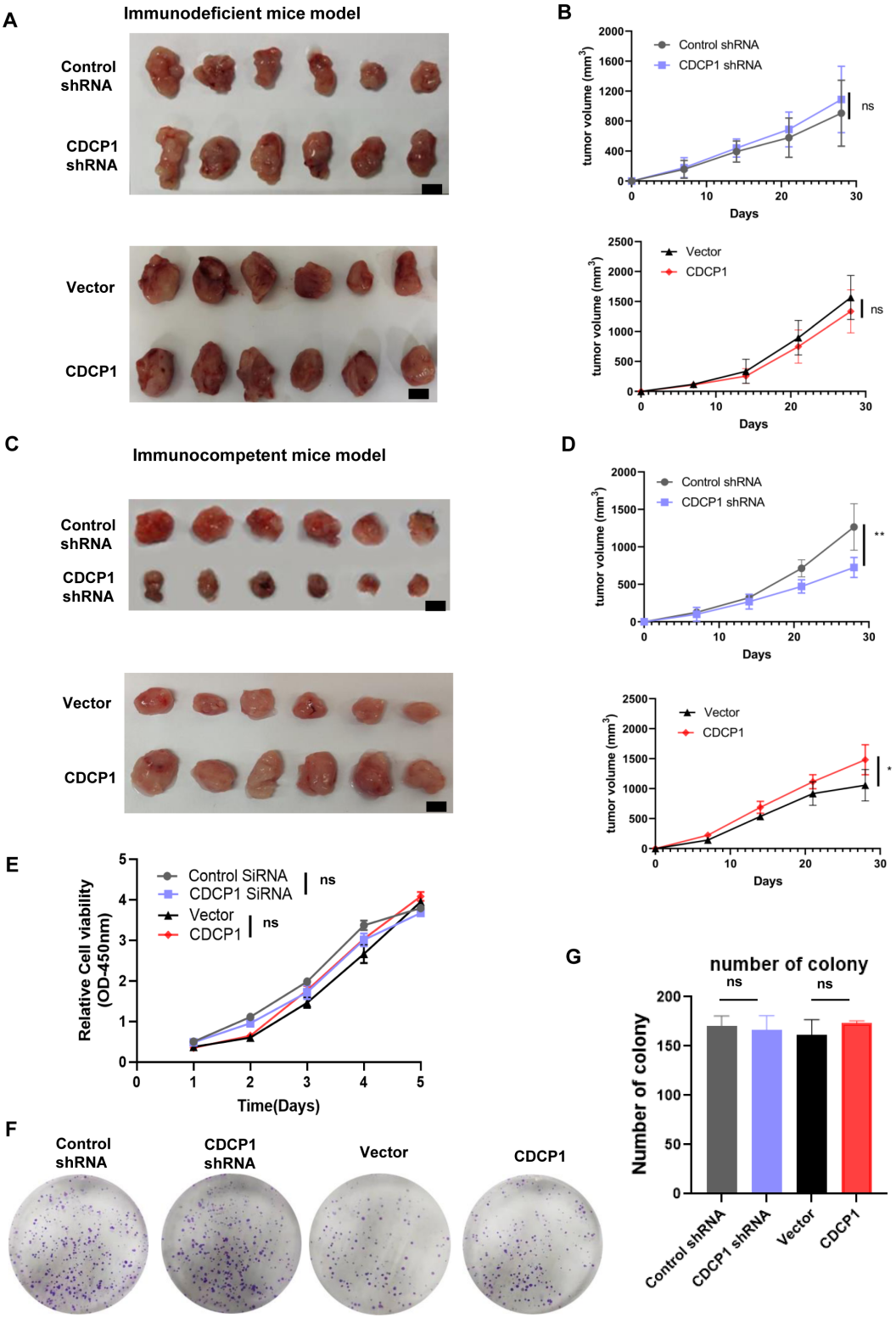

Figure 2 The expression level of CDCP1 effected xenograft tumor growth in an immune-dependent manner. (A, B) Subcutaneous injection of control cells, CDCP1 knockdown, and CDCP1 overexpression U14 cells into 5-week-old female BALB/c-nu immunodeficiency mice (n=8 for each group). Representative images are shown in A, B. The line graph depicts the tumor growth curve of mice. Scale bar:50 mm. Values are presented as the mean±SD. *p<0.05, **p<0.01. (C, D) Subcutaneous injection of control cells, CDCP1 knockdown, and CDCP1 overexpression U14 cells into 6-week-old female C57BL/6J immunocompetent mice (n=8 for each group). Representative images are shown in (C, D). The line graph shows the tumor growth curve of mice. Scale bar:50 mm. Values are presented as the mean±SD ns, not significant. *p<0.05, **p<0.01. (E–G) Proliferation of control cells, CDCP1 knockdown, and CDCP1 overexpression U14 cells analyzed by CCK-8 assay (E) and colony formation assay (F, G). Data represent at least three independent experiments. Values are presented as the mean±SEM. Significance was determined using one way ANOVA test, *p<0.05, **p<0.01. ANOVA, analysis of variance; ns, not significant.

in immunocompetent mice compared with control cells, while CDCP1 overexpression had the opposite effect (figure 2B,D). These results indicate that CDCP1 plays a critical role in promoting tumor growth in vivo in an immune-dependent manner.

To elucidate the mechanisms underlying the effects of CDCP1 on tumor growth, we evaluated the proliferation of control cells, CDCP1 knockdown, and overexpression U14 cells using CCK-8 and colony formation assays. Figure 2E shows that the proliferation level of U14 cells themselves is not affected by knockdown or overexpression of CDCP1. Similarly, the colony formation assays show that the long-term proliferation capacity of U14 cells themselves is not affected by the knockdown or overexpression of CDCP1 (figure 2F,G). This result indicates that CDCP1 does not affect the proliferation level of tumor cells themselves, further suggesting that the influence of CDCP1 on in vivo tumor growth occurs through immunological pathways.

Analysis of different expression levels of CDCP1 affection on tumor-infiltrating immune cells in immunocompetent mouse models

To investigate the effect of CDCP1 interference on tumor-infiltrating immune cells, we established a murine tumor model by subcutaneous injection of U14 tumor cells with different levels of CDCP1 expression into immunocompetent C57 mice. Tumors were harvested for flow cytometry analysis on day 10 after tumor palpation.

Figure 3A shows the frequencies of different types of tumor infiltrating immune cells were analyzed. Compared with the control group, there were no significant changes in the numbers of CD45+leucocytes, CD11B+myeloid cells, neutrophils, macrophages, CD3+T cells, and CD4+T cells in either the CDCP1 knockdown or CDCP1 overexpression groups. Compared with the control group, the subcutaneous tumors implanted with CDCP1 knockdown U14 tumor cells showed a significant increase in the infiltration of CD8+T cells, with a notable increase in the proportion of GZMB+IFNγ+ cytotoxic T cells. In contrast, the proportion of CD25+FOXP3+ regulatory T cells (Tregs) decreased significantly. Conversely, in the subcutaneous tumors implanted with CDCP1-overexpressing U14 tumor cells, the pattern of immune cell infiltration was completely opposite. These results suggest that the effect of CDCP1 on in vivo tumor growth may be mediated through its influence on the functionality of tumor-infiltrating T lymphocytes.

Therefore, we established co-culture systems of murine and human tumor cell lines with corresponding T cells of the same species in vitro. We observed whether interfering with the expression level of CDCP1 on tumor cells directly affects the functional status of T cells in the co-culture system.

After 48 hours of co-culture with activated T cells (tumor-to-T cell ratio=1:10), the cell survival rates of murine U14 tumor cells and human SiHa tumor cells with different levels of CDCP1 expression were measured (online supplemental figure 2A). In both the murine cervical cancer tumor cell-T cell co-culture system and the human tumor cell-T cell co-culture system, compared with the control group, the survival rate of CDCP1 knockdown tumor cells under the specific cytotoxic effect of T cells was significantly decreased compared with the control group, while the survival rate of CDCP1 overexpressing tumor cells was increased (online supplemental figure 2B,C).

Meanwhile, we analyzed the activation level of T cells in the co-culture system by flow cytometry. Murine T cells were co-cultured with different CDCP1 levels of U14 cells at a ratio of 2.5:1 for 16 hours. Consistent with the specific tumor-killing effect, the frequency of IFNγ+ and GZMB+-cytotoxic T cells, which are the main effectors of tumor killing, was highest when co-cultured with CDCP1 knockdown tumor cells and significantly lower when co-cultured with tumor cells overexpressing CDCP1 (online supplemental figure 2D). In the co-culture system of human tumor cells and T cells, we simultaneously observed the differences in CD107a+CD137+ activated CD8+ T cells. Similarly, the frequencies of IFNγ+ and GZMB+cytotoxic T cells as well as CD107a+CD137+ CTL were both highest when co-cultured with CDCP1 knockdown tumor cells and significantly lower when co-cultured with tumor cells overexpressing CDCP1 (online supplemental figure 2E,F).

Collectively, our results demonstrate that CDCP1 on tumor cells affects the composition and function of tumor-infiltrating immune cells in immunocompetent mouse models and promote an antitumor immune response characterized by increased cytotoxic activity of CTLs and decreased frequency of immunosuppressive Tregs. These results highlight the importance of CDCP1 as a potential therapeutic target for modulating the tumor immune microenvironment in cancer therapy.

CDCP1 impairs T cell-mediated antitumor immunity via CD6

Based on previous research, CD6 is a surface glycoprotein on T cells that regulates T cell activation through interaction with its ligand.[51 52] CDCP1, which has been observed to be upregulated in numerous tumors, has been identified as the second ligand of CD6.[53] We hypothesize that in cervical cancer, the regulatory role of CDCP1 on the function of tumor-infiltrating T cells is mediated through its interaction with CD6. Therefore, we investigated whether CD6 blockade can abolish the effects of CDCP1 on tumor-infiltrating T cells.

Previous studies have highlighted the potential of CD6 as an immunotherapy target. Similarly, our experimental results sshow that injection of anti-CD6 monoclonal antibody into immunocompetent mice significantly inhibits tumor growth. In the presence of anti-CD6, the effect of CDCP1 knockdown on tumor growth is not significant compared with the control group (figure 4A,B).

Furthermore, flow cytometric analysis was performed to evaluate changes in the functionality of infiltrating T cells in the tumor. The results showed that anti-CD6

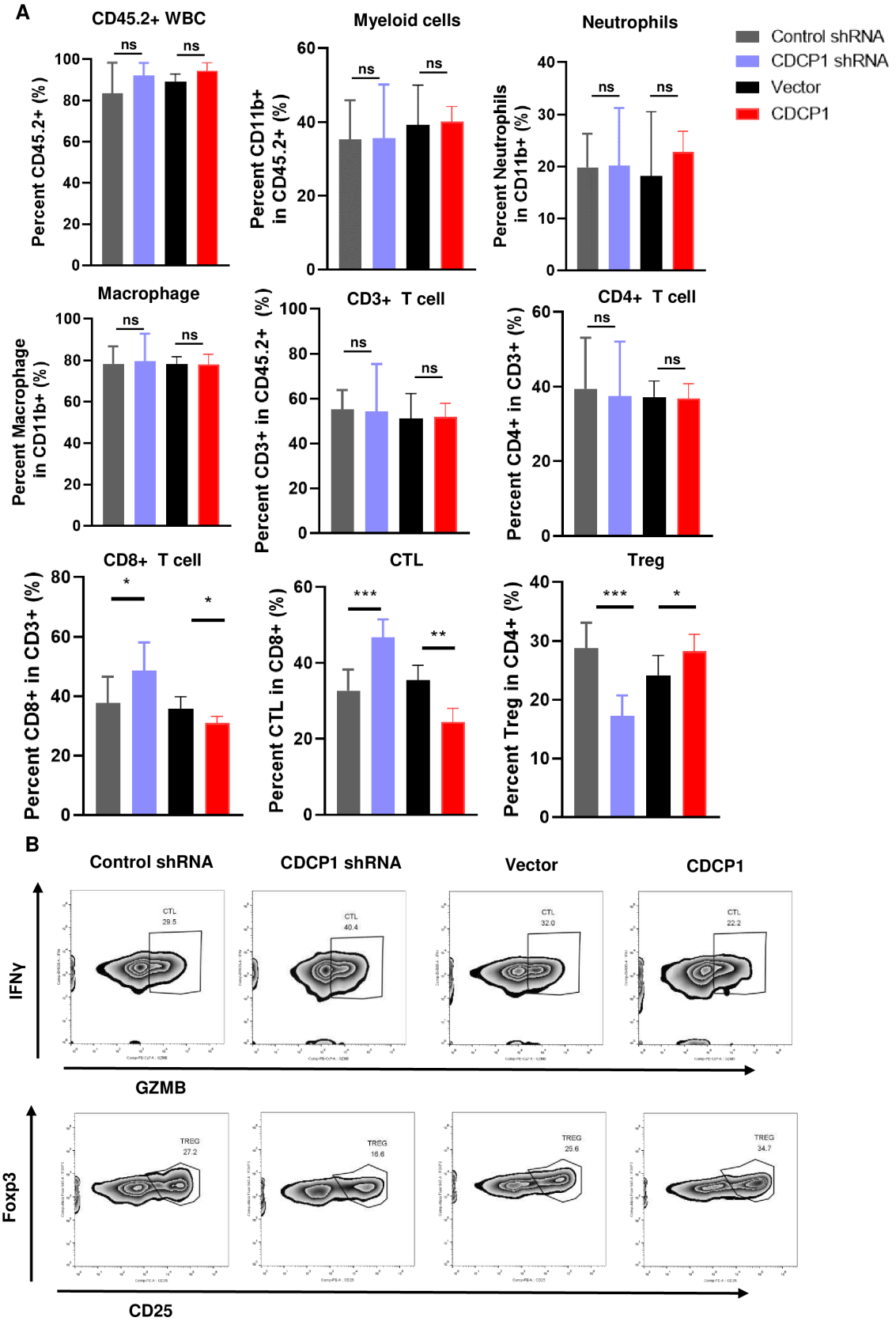

Figure 3 Analysis of different expression level of CDCP1 affection on tumor-infiltrating immune cells in immunocompetent mice models. (A) Control cells, CDCP1 knockdown and overexpression U14 cells formatted xenograft tumors in immunocompetent mice. Tumors were harvested and analyzed using flow cytometry. Myeloid cells, neutrophils, macrophages (n=4) and T cells (n=4) were analyzed. Statistics were performed using a Student's t-test between groups. *p<0.05, **p<0.01, ***p<0.001. (B) Representative flow cytometry images frequencies of IFNγ+GZMB+ CTLs, Foxp3+CD25+Treg between groups. ns, not significant.

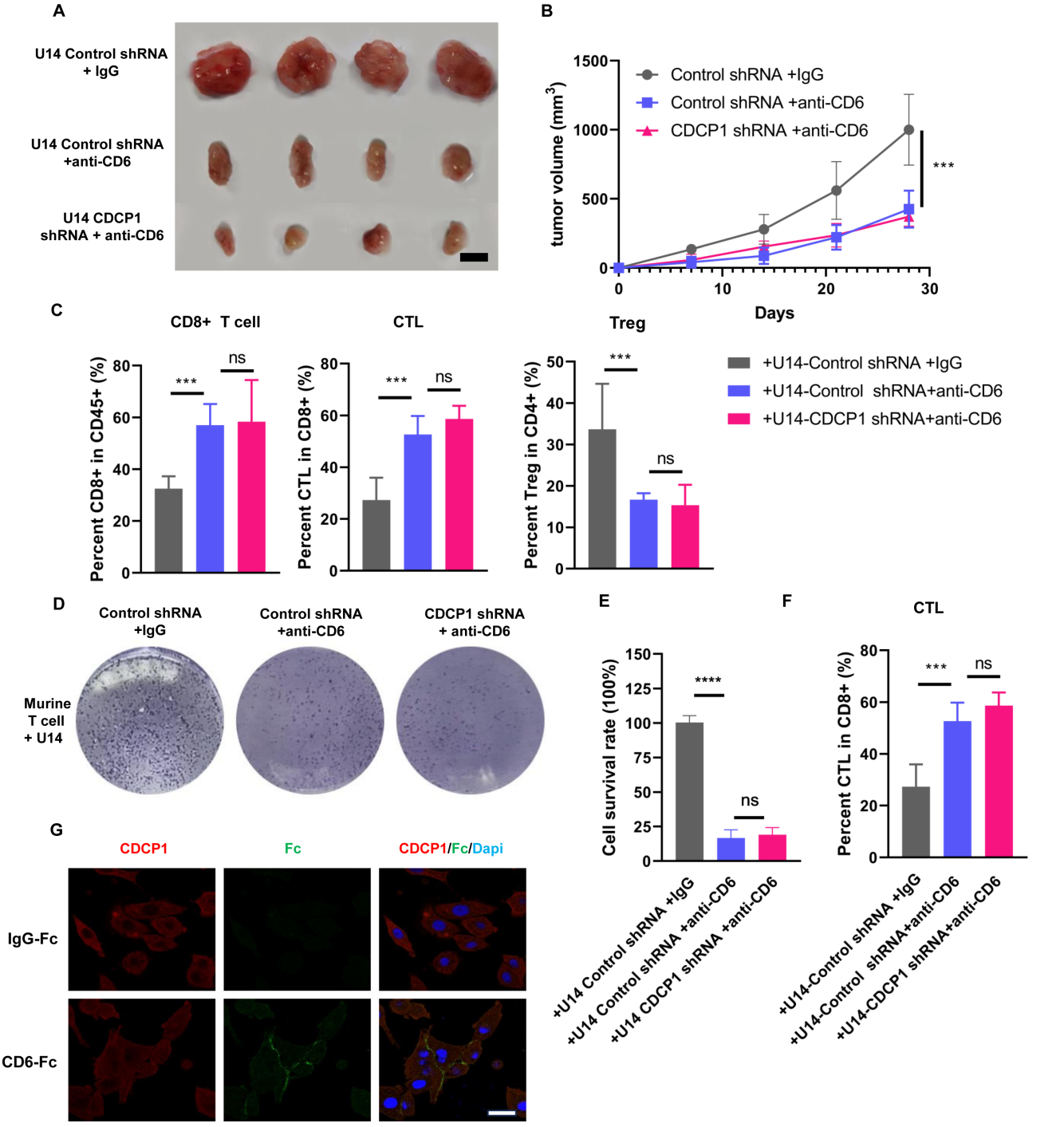

Figure 4 CDCP1 impair T-cell-mediated antitumor immunity through CD6. (A, B) Subcutaneous injection of control and CDCP1 knockdown U14 cells into 6-week-old female C57BL/6J immunocompetent mice (n=4 for each group). When tumors reaching a volume of 100 mm^3, mice were randomly divided into groups and were intravenously injected with anti-CD6 monoclonal antibody or IgG control. Representative images are shown in A. Scale bar:50 mm. (B) The line graph illustrates the tumor growth curve of mice. Data are presented as the mean±SD. *p<0.05, **p<0.01, ***p<0.001, ****p<0.0001. (C) Frequencies of CD8+T cell, IFNγ+ GZMB+ CTLs and Foxp3+CD25+Treg in xenografts were analyzed. Data are presented as the mean±SD. Statistics were performed using a Student's t-test between groups. *p<0.05, **p<0.01, ***p<0.001. (D–F) Murine U14 cells with different CDCP1 level were co-cultured with activated T cells (tumor-to-T cell ratio=1:2) for 48 hours with anti-CD6 monoclonal antibody or IgG control in vitro. Cells were subjected to crystal violet staining. Relative fold ratios of surviving tumor cell intensities are shown in E. Frequencies of IFNγ+ and GZMB+CTLs were quantified, as in F. Data are presented as the mean±SD. Statistics were performed using a Student's t-test between groups. ns, not significant,***p<0.001. (G) Representative immunofluorescence labeling images indicated the interaction between CDCP1 and exogenous CD6 protein. Following incubation with recombinant human CD6-Fc fusion protein or human IgG, CDCP1 was diffusely distributed across the membrane and cytoplasm of SiHa cells (red signal). In the group treated with the exogenous CD6-Fc recombinant protein, CDCP1 binding to CD6 resulted in Fc staining positivity on the SiHa cell membrane (green signal). Scale bar: 5 μm.

monoclonal antibody increased the proportion of infiltrating CD8+T cells within the tumor compared with the control group, with a significant increase in the proportion of IFNγ+ GZMB+ cytotoxic T cells. Conversely, the proportion of inhibitory Tregs was significantly reduced. Notably, under the influence of anti-CD6, the effect of CDCP1 knockdown on the functionality of tumor-infiltrating T cells was not observed (figure 4C).

Meanwhile, we investigated whether CD6 blockade directly affects the interaction between tumor cells and T cells in an in vitro co-culture model. Compared with the control group, the addition of anti-CD6 in the co-culture system significantly increased the cytotoxicity of T cells against U14 tumor cells. Flow cytometric analysis revealed a significant increase in the proportion of activated cytotoxic T cells. However, under conditions of CD6 blockade conditions, the effect of CDCP1 knockdown tumor cells on the co-cultured T cells was minimal (figure 4D–F).

Taken together, our results showed that the CDCP1 attenuated T cell-mediated antitumor immunity through CD6.

CDCP1 binds to CD6 and inhibits the JAK-STATs signaling

Using immunofluorescence (IF) labeling techniques,[46] we observed that CDCP1 binds to externally added CD6 protein in the human tumor cell line SiHa, compared with the control group (figure 4G). This finding is consistent with previous literature identifying CDCP1 as a second ligand for CD6.[53] We then investigated into how CDCP1 on the surface membrane of tumor cells affects T cell function through the T cell receptor CD6. To elucidate the signaling pathways affected by the interaction between CDCP1 and CD6 in T cells, RNA-seq analysis was performed on T cells co-cultured with CDCP1 overexpressing U14 cells versus control U14 cells, both stimulated with anti-CD3/CD28 antibodies for 24 hours. On downstream Kyoto Encyclopedia of Genes and Genomes (KEGG) pathway analysis of differentially expressed genes between the two groups, downstream pathways related to tumor immunity such as the JAK-STAT signaling pathway and cytokine-cytokine receptor interaction were found to be suppressed in T cells co-cultured with CDCP1 overexpressing U14 tumor cells (figure 5A). Gene set enrichment analysis further indicated a strong depression of the JAK-STAT signaling pathway in CDCP1 overexpressing U14 co-cultured T cells (figure 5B). In addition, we performed qRT-PCR to identify the activation of JAK-STAT pathway in the T cells co-cultured with U14 tumor cells with different levels of CDCP1. Compared with the control group, the target genes of the JAK-STAT signaling pathway, including Ifnγ, Ifngr1, and Il2, were downregulated, while Il6 and Il10 were upregulated, confirming the suppression of the JAK-STAT signaling pathway in T cells co-cultured with CDCP1 overexpressing U14 cells (figure 5C). Based on the literature review, the JAK-STAT signaling pathway in T cells was found to regulate the differentiation and function of CTLs by controlling the transcription and expression of immune-related genes.[54–56] Suppression of the JAK-STAT signaling pathway reduced the production of cytotoxic molecules such as GZMB and IFNγ.

In addition, suppression of the JAK-STAT signaling pathway can regulate the production of cytokine and the receptor signal transduction, leading to transcriptional production of IL2 or IL10. This increases the infiltration and activation status of immunosuppressive cells such as regulatory T cells (TREGs) within the tumor microenvironment, thereby impairing antitumor immunity.

At the same time, the expression levels of JAK-STAT signaling activation proteins, such as pJAK1, pSTAT1, and pSTAT3, were assessed in T cells co-cultured with CDCP1 knockdown U14 cells and control U14 cells. In T cells co-cultured with CDCP1 knockdown cells, the levels of phosphorylated JAK1, STAT1, and STAT3 proteins increased over time after activation compared with controls. However, the total protein levels of JAK1, STAT1, and STAT3 remained unchanged (figure 5D). These results suggest that the influence of CDCP1 on the JAK-STAT signaling pathway in T cells may be mediated by modulating the phosphorylation of key molecules such as JAK1, STAT1, and STAT3.

Based on our previous experiments, we have found that the effect of CDCP1 on T cell function requires mediation by the CD6 receptor on T cells. Next, we investigated whether the effect of CDCP1 on JAK-STAT signaling in T cells is mediated by CD6. We added anti-CD6 mAb to the co-culture system to block the interaction between CDCP1 on tumor cells and CD6 on T cells. The results showed that overexpression of CDCP1 significantly reduced the phosphorylation levels of JAK1, STAT1, and STAT3 compared with the control group. However, after the addition of anti-CD6 mAb, CDCP1 overexpression was unable to reduce the phosphorylation levels of JAK1, STAT1, and STAT3 in T cells (figure 5E).

To identify the interaction of CD6 and JAK1 inside the T cell, the CD6 protein was tagged by FLAG in the CD8+T cells from the spleen of the C57 mice and immunoprecipitation was performed using FLAG antibody or control IgG. The experiment demonstrated an interaction between CD6 and JAK1 within the T cells (figure 5F).

We further investigated whether the CDCP1 inhibitor 8PN[48] activates JAK-STAT signaling in T cells. T cells co-cultured with CDCP1-overexpressing U14 cells were pretreated with or without 8PN and then activated with CD3 and CD28 antibodies for 30 min. Treatment with 8PN significantly downregulated the expression of CDCP1 in tumor cells as described in previous literature.[48] Consistent with CDCP1 downregulation, the phosphorylation of JAK1-STAT1/3 was observed in T cells of both CDCP1 overexpressing group and control group. These results suggest that CDCP1 inhibitor 8PN activates the JAK1-STAT1/3 signaling pathway in T cells (figure 5G).

Most importantly, there experiment elucidated the effect of CDCP1 on tumor cells binds to CD6 and inhibits JAK-STATs signaling of T cells.

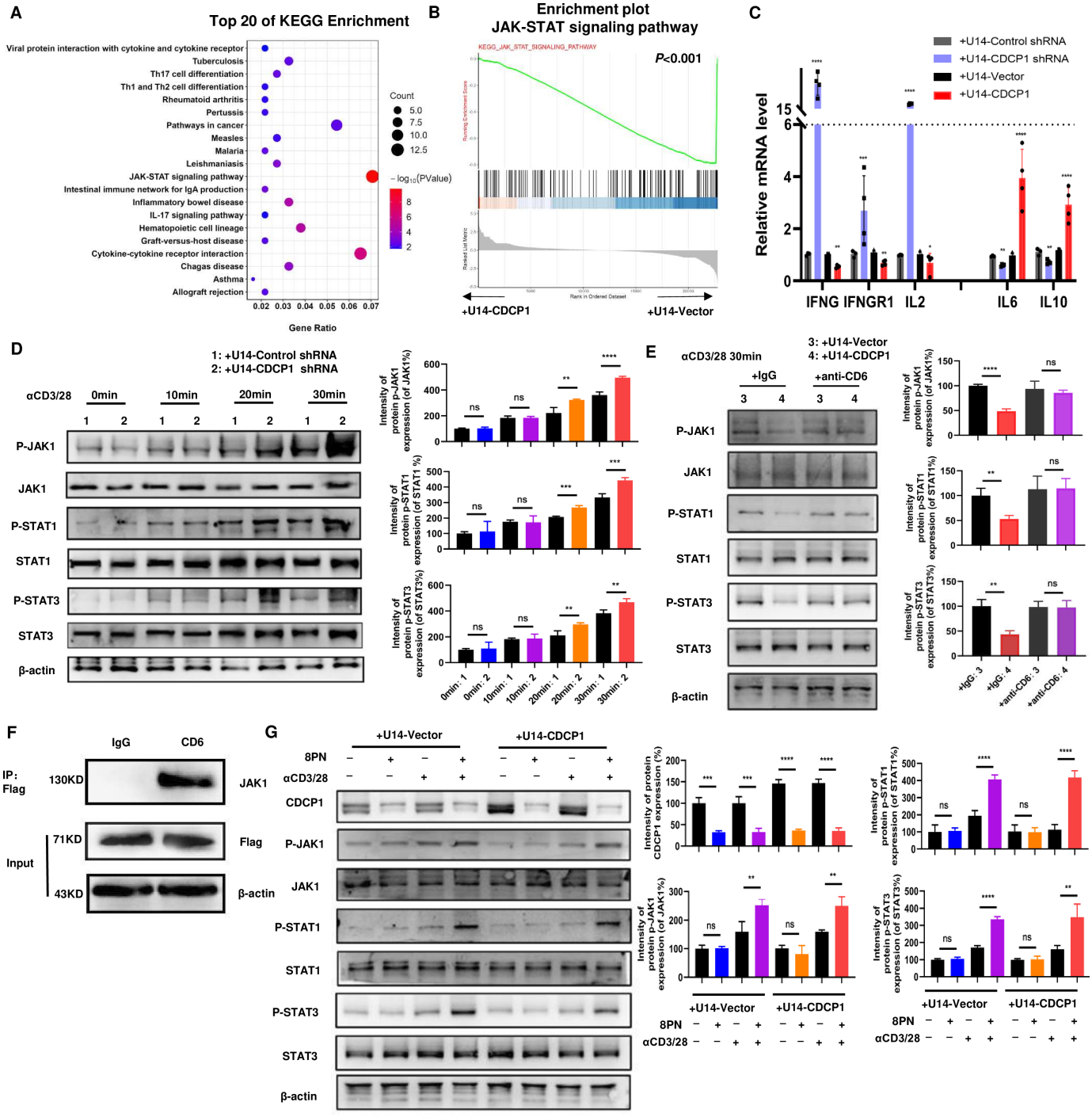

Figure 5 CDCP1 inhibits the JAK-STATs signaling of T cells. (A) Kyoto Encyclopedia of Genes and Genomes (KEGG) analysis of RNA-seq data of active T cells co-cultured with of CDCP1 overexpressing U14 cell vs control U14 cells for 24 hours. (B) GSEA analysis of the differentially expressed genes (from RNA-seq datasets) involved in the suppression of JAK-STAT signaling pathway in T cells co-cultured with CDCP1 overexpressing U14 cells compared with T cells co-cultured with control U14 cells. p<0.001. (C) qPCR validation of the expression of genes downstream JAK-STAT signaling pathway in active T cells co-cultured with different CDCP1 expression level U14 cells. (D) The activation of the JAK-STAT pathway was assessed in the lysates of T cells co-cultured with control and CDCP1 knockdown U14 cells, following stimulation with anti-CD3 and anti-CD28 antibodies for 10–30 min. (E) The activation of the JAK-STAT pathway was assessed in the lysates of T cells co-cultured with control and CDCP1-overexpressing U14 cells, with or without anti-CD6 blockade. (F) Immunoprecipitation assay identified the interaction between CD6 and JAK1 in T cells. Murine T cell were transfected with CD6-3xFlag plasmid. Cell lysates were immunoprecipitated with Flag antibody and analyzed by immunoblot with anti-JAK1 and anti-Flag. (G) CDCP1 inhibitor 8PN activates the JAK1-STAT1/3 signaling pathway in T cells. After pretreated with 8PN or DMSO for 24 hours, the activation of the JAK-STAT pathway was assessed in the lysates of T cells co-cultured with control and CDCP1-overexpressing U14 cells. Significance was determined using Student's t-test. *p<0.05, **p<0.01, ***p<0.001, ****p<0.0001. ns, not significant.

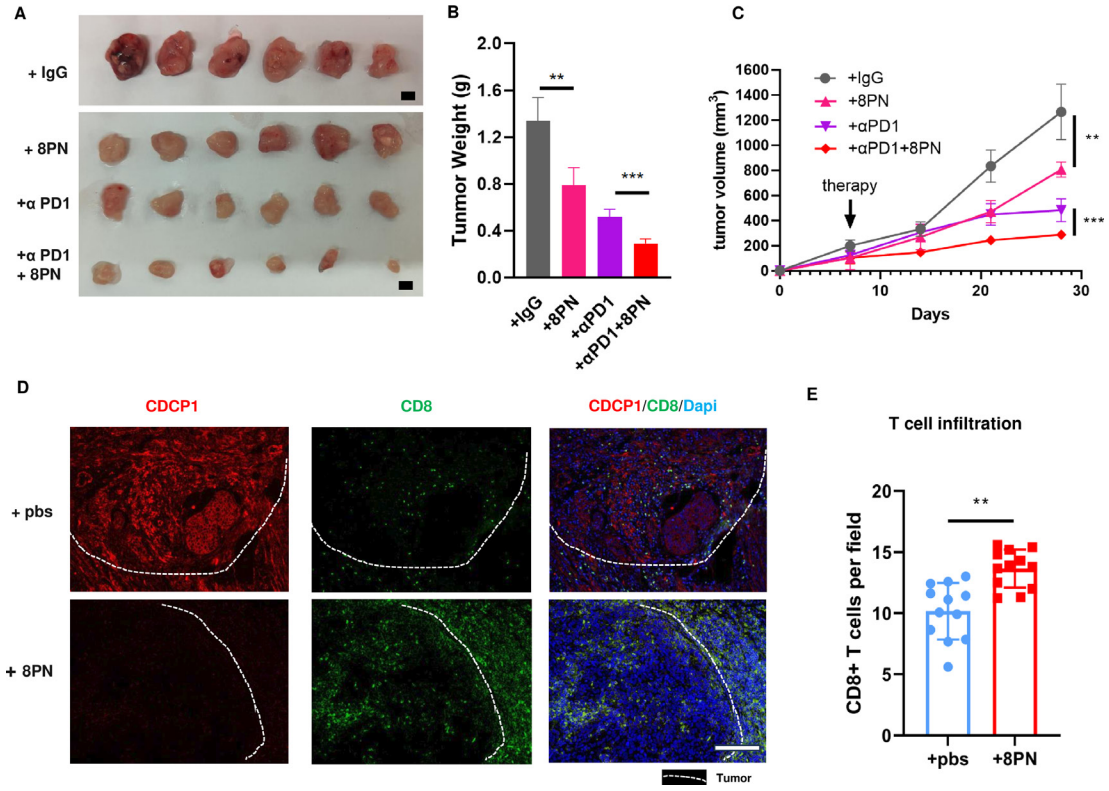

Figure 6 Targeting CDCP1 suppressed cervical cancer growth. (A–C) Subcutaneous injection of U14 cells into 6-week-old female C57BL/6J immunocompetent mice. When tumors reaching a volume of 100 mm^3, mice were randomly divided into groups and were intravenously injected with anti-CD6 monoclonal antibody, anti-PD1 antibody, anti-CD6 antibody plus anti-PD1 antibody or IgG control. Representative images are shown in A. Scale bar: 50 mm. (B) of the resected tumor at day 28 after inoculation. Data are representative of two independent experiments. Values are presented as the mean±SEM. (C) The line graph illustrates the tumor growth curve of mice. Values are presented as the mean±SEM. Statistical significance was determined by Student's t-test. **p<0.01, ***p<0.001. (D–E) The infiltration of CD8+T cell in cervical cancer xenograft specimen of CDCP1 inhibitor 8PN treatment group and control group. (D). Representative immunofluorescence images of two groups. White dashed line marks the boundary between the tumor tissue and the adjacent non-cancerous tissue. Scale bar: 50 μm. (E). Data are shown as mean±SEM. Statistical significance was determined by Student's t-test. ns, not significant. *p<0.05, **p<0.01, ***p<0.001. ns, not significant.

Targeting CDCP1 suppressed cervical cancer growth

To investigate the potential of CDCP1 as an immune checkpoint target for cervical cancer therapy, we used the CDCP1 inhibitor, 8PN, aiming to evaluate its therapeutic efficacy in an immunocompetent model.

We initiated drug treatment when the subcutaneous tumors reached approximately 100 mm^3 (around day 10). Experimental results showed that the CDCP1 inhibitor 8PN significantly suppressed the in vivo growth of cervical cancer cells and tumor weight (figure 6A–C). In addition, combined treatment with anti-PD1 monoclonal antibody showed a more pronounced inhibitory effect on tumor growth.

Next, we used IF to examine the levels of tumor-infiltrating T cells in subcutaneous tumor samples. The results showed a significant increase in the levels of infiltrating T cells in the group treated with the CDCP1 inhibitor 8PN compared with the control group (figure 6D–E). This suggests that the inhibition of tumor growth in vivo is most likely due to the enhancement of antitumor immunity within the microenvironment facilitated by CDCP1 inhibition.

Collectively, our findings provide robust evidence for the potential of CDCP1 to enhance antitumor immunity and improve clinical outcomes. Targeting CDCP1 to enhance CD8+T cell-mediated cytotoxicity may prove to be a promising immunotherapeutic approach in the treatment of cervical cancer.

DISCUSSION

In this study, we investigated the potential of CDCP1 as an immunotherapeutic target in cervical cancer and demonstrated its tumor overexpression and association with poor prognosis and low CTL infiltration in both the TCGA-CESC and FAH-SYSU cohorts. Using xenograft models in both immunocompetent and immunodeficient mice, we found that CDCP1 deficiency suppressed tumor growth in immunocompetent mice, highlighting the role of immune cells in mediating the effects of CDCP1 on tumor growth. CDCP1 overexpression was associated with decreased CTL infiltration and increased regulatory T cells (Tregs) in tumors, while the opposite was observed with low CDCP1 expression.

Co-culture experiments further confirmed that CDCP1 on tumor cells directly interacts with T cells in the tumor microenvironment, influencing their differentiation and function. This study provides the first experimental evidence of CDCP1's interaction with T cells in cervical cancer.

Furthermore, we investigated the mechanisms by which CDCP1 induces immune evasion in cervical cancer. The gene expression data and detection of protein phosphorylation levels in figure 5 showed that overexpression of CDCP1 inhibited the JAK-STAT signaling of co-cultured T cells. This is a classical pathway that regulates T cell activation by inducing the expression of cytokines and growth factors. We have thus demonstrated a novel mechanism of CDCP1 in the suppression of T cell activity.

CD6 is a type I transmembrane glycoprotein ranging of 105–130 kDa and belongs to the ancient and highly conserved scavenger receptor cysteine-rich superfamily. CD6 is exclusively expressed by lymphocytes, including most mature T cells and approximately 50% of NK cells.[57 58] Previous studies have implicated CD6 functioned in T cell activation and immune responses. While the inhibitory function of CD5 is well established, it remains controversial regarding whether CD6 may have similar or antagonistic roles in T cell signaling.[59 60] CD6 is involved in lymphocyte activation, proliferation, and survival through interactions with its endogenous ligands. Previous studies have identified two ligands for CD6: CD166/Activated Leukocyte Cell Adhesion Molecule (ALCAM)[61] and CD318, also known as CDCP1.[53]

ALCAM, a member of the immunoglobulin superfamily, is widely expressed in various tissues, including endothelial and epithelial cells and APCs.[62] The CD6/ALCAM interaction plays a multifaceted role in T cell activation and function. Initially, CD6 colocalizes with the TCR/CD3 complex and binds to ALCAM expressed on APCs. This interaction strengthens the immune synapse, thereby prolonging T cell/APC interaction time, which is essential for optimal activation of cytotoxic T cells.[63] Costimulation of CD3 on PBMCs with ALCAM enhances T cell activation.

However, our experimental results have shown for the first time that CDCP1 binds to CD6 and inhibits T cell activation, suggesting that CDCP1, unlike ALCAM, may exert an inhibitory effect on T cell activity. ALCAM and CDCP1 are both ligands of CD6, but their effects on T cell regulation on binding to CD6 are opposite. This leads us to consider that the activation of T cells, facilitated by the binding of ALCAM to CD6 on APCs, may be a consequence of antigen recognition by the TCR/CD3 complex. It raises the question of whether the high expression of CDCP1 on tumor cells competes with ALCAM for CD6 binding, disrupting the binding of ALCAM to CD6, thereby inhibiting costimulation of CD3 on PBMCs with ALCAM, enhancing T cell activation and downstream T-cell activation, and promoting tumor immune evasion. However, this hypothesis requires further experimental validation in the future.

Finally, we evaluated the therapeutic effect of CDCP1 inhibitor 8PN treatment in a cervical cancer mouse model. Our results showed that 8PN effectively reduced CDCP1 expression both in vitro and in vivo (figures 5G and 6E), indicating its role as a CDCP1 inhibitor.

While 8PN has been shown to target CDCP1, we recognize the possibility of off-target effects. As a phytoestrogen analog, previous studies have reported that 8PN may affect the proliferative capacity of breast cancer cells through estrogen receptors (ER) on the tumor cell membrane.[64] In cervical cancer, den Boon JA *et al* found that ER expression was significantly lower in cervical cancer tissues compared with normal tissues, with ER primarily localized primarily to stromal fibroblasts rather than tumor cells.[65] This suggests that the direct estrogen-like effects of 8PN on cervical cancer cells may be limited. However, 8PN could potentially affect tumor growth through its action on ER-expressing fibroblasts in the tumor stroma.

Interestingly, in our mouse model, 8PN was observed to enhance CD8+T cell infiltration into subcutaneous tumors (figure 6D,E), suggesting that 8PN may also modulate antitumor immunity. Given the complex role of estrogen in cervical cancer, which remains inconclusive, further studies are needed to clarify these mechanisms. In addition, the combination of PD-1 monoclonal antibody with CDCP1 inhibition resulted in enhanced tumor suppression (figure 6A–C), suggesting that targeting CDCP1 may provide therapeutic benefit. These findings highlight the potential of CDCP1 inhibition as an immunotherapeutic strategy, but further research is warranted to fully understand its mechanisms and optimize its clinical application.

Overall, our study provides valuable insights into the potential role of CDCP1 as an immunotherapeutic target in the treatment of cervical cancer. Further investigation is warranted to elucidate the underlying mechanisms and to validate the efficacy of CDCP1-targeted immunotherapy in the clinical setting.

Acknowledgements We thank the Pathology Department of the First Affiliated Hospital of Sun Yat-sen University for supporting the histological identification.

Contributors Conception: HH, YP, QM, JunxiuL and SY; Methodology and investigation: HH, YP, QM, CZ, YLiao and QD; Resources: JH, JieL, TL and YZ; Formal analysis and visualization: HH, QM, QZ and LY; Writing—original draft: HH, YP and QM; Writing—review and editing: HH, YP, YLiang, WW and CYP; Supervision: YLiang, WW, CYP, JunxiuL and SY; Project administration: HH, JunxiuL and SY; Funding acquisition: JunxiuL and SY. Guarantor: SY. AI was used to polish this article.

Funding The National Natural Science Foundation of China (82273365, 82072874 to SY, 82072884, 81872128 to JieL; 82303920 to QD; 82303390 to YC; 82403524 to CZ), National Key R&D Program of China (2022YFC2704201 to SY), Science and Technology Plan of Guangdong Province (2023A0505050102 to SY), Guangzhou Science and Technology Program (2024B03J1336 to SY), Xisike-Hengri Oncology Research Program (Y-HR2022MS-0730 to JieL), Technology Research Project of Zhongshan City (2022B3009 to YC and JunxiuL),Sun Yat-sen University Clinical Research Foundation of 5010 Project (2017006 to SY).

Competing interests None declared.

Patient consent for publication Not applicable.

Ethics approval Clinical Ethics Committee of the Experimental Animal Center, Sun Yat-sen University, approval ID:2023000209.

Provenance and peer review Not commissioned; externally peer reviewed.

Data availability statement Data are available on reasonable request.

Author note guarantor: Shuzhong Yao

ORCID iDs
Hua Huang http://orcid.org/0000-0002-1713-8597
Qiqiao Du http://orcid.org/0000-0003-4053-1044
Junxiu Liu http://orcid.org/0000-0002-7892-6343

REFERENCES

1 Sung H, Ferlay J, Siegel RL, *et al*. Global Cancer Statistics 2020: GLOBOCAN Estimates of Incidence and Mortality Worldwide for 36 Cancers in 185 Countries. *CA Cancer J Clin* 2021;71:209–49.
2 Ferlay J, Ervik M, Lam F, *et al*. Cancer observatory: cancer today. Lyon, France: International Agency for Research on Cancer; 2024.8. Available: https://gco.iarc.who.int/today
3 WHO. Cervical cancer. 2023. Available: https://www.who.int/zh/news-room/fact-sheets/detail/cervical-cancer
4 Poddar P, Maheshwari A. Surgery for cervical cancer: consensus & controversies. *Indian J Med Res* 2021;154:284–92.
5 Vavassori A, Riva G, Spoto R, *et al*. High precision radiotherapy including intensity-modulated radiation therapy and pulsed-dose-rate brachytherapy for cervical cancer: a retrospective monoinstitutional study. *J Contemp Brachytherapy* 2019;11:516–26.
6 Lorusso D, Petrelli F, Coinu A, *et al*. A systematic review comparing cisplatin and carboplatin plus paclitaxel-based chemotherapy for recurrent or metastatic cervical cancer. *Gynecol Oncol* 2014;133:117–23.
7 Kitagawa R, Katsumata N, Shibata T, *et al*. Paclitaxel Plus Carboplatin Versus Paclitaxel Plus Cisplatin in Metastatic or Recurrent Cervical Cancer: The Open-Label Randomized Phase III Trial JCOG0505. *J Clin Oncol* 2015;33:2129–35.
8 Shrestha AD, Neupane D, Vedsted P, *et al*. Cervical Cancer Prevalence, Incidence and Mortality in Low and Middle Income Countries: A Systematic Review. *Asian Pac J Cancer Prev* 2018;19:319–24.
9 Mackay HJ, Wenzel L, Mileshkin L. Nonsurgical management of cervical cancer: locally advanced, recurrent, and metastatic disease, survivorship, and beyond. *Am Soc Clin Oncol Educ Book* 2015;e299–309.
10 Serkies K, Jassem J. Systemic therapy for cervical carcinoma - current status. *Chin J Cancer Res* 2018;30:209–21.
11 Orbegoso C, Murali K, Banerjee S. The current status of immunotherapy for cervical cancer. *Rep Pract Oncol Radiother* 2018;23:580–8.
12 Ferrall L, Lin KY, Roden RBS, *et al*. Cervical Cancer Immunotherapy: Facts and Hopes. *Clin Cancer Res* 2021;27:4953–73.
13 Chung HC, Ros W, Delord J-P, *et al*. Efficacy and Safety of Pembrolizumab in Previously Treated Advanced Cervical Cancer: Results From the Phase II KEYNOTE-158 Study. *J Clin Oncol* 2019;37:1470–8.
14 Oyouni AAA. Human papillomavirus in cancer: Infection, disease transmission, and progress in vaccines. *J Infect Public Health* 2023;16:626–31.
15 Lin D, Kouzy R, Abi Jaoude J, *et al*. Microbiome factors in HPV-driven carcinogenesis and cancers. *PLoS Pathog* 2020;16:e1008524.
16 Yuan Y, Cai X, Shen F, *et al*. HPV post-infection microenvironment and cervical cancer. *Cancer Lett* 2021;497:243–54.
17 Vari F, Arpon D, Keane C, *et al*. Immune evasion via PD-1/PD-L1 on NK cells and monocyte/macrophages is more prominent in Hodgkin lymphoma than DLBCL. *Blood* 2018;131:1809–19.
18 He X, Xu C. Immune checkpoint signaling and cancer immunotherapy. *Cell Res* 2020;30:660–9.
19 Chen L, Han X. Anti-PD-1/PD-L1 therapy of human cancer: past, present, and future. *J Clin Invest* 2015;125:3384–91.
20 Gainor JF, Shaw AT, Sequist LV, *et al*. EGFR Mutations and ALK Rearrangements Are Associated with Low Response Rates to PD-1 Pathway Blockade in Non-Small Cell Lung Cancer: A Retrospective Analysis. *Clin Cancer Res* 2016;22:4585–93.
21 Yi M, Zheng X, Niu M, *et al*. Combination strategies with PD-1/PD-L1 blockade: current advances and future directions. *Mol Cancer* 2022;21:28.
22 Gupta S, Kumar P, Das BC. HPV: Molecular pathways and targets. *Curr Probl Cancer* 2018;42:161–74.
23 Li C, Hua K. Dissecting the Single-Cell Transcriptome Network of Immune Environment Underlying Cervical Premalignant Lesion, Cervical Cancer and Metastatic Lymph Nodes. *Front Immunol* 2022;13.
24 Gu M, He T, Yuan Y, *et al*. Single-Cell RNA Sequencing Reveals Multiple Pathways and the Tumor Microenvironment Could Lead to Chemotherapy Resistance in Cervical Cancer. *Front Oncol* 2021;11:753386.
25 Chong Z-X, Ho W-Y, Yeap S-K, *et al*. Single-cell RNA sequencing in human lung cancer: Applications, challenges, and pathway towards personalized therapy. *J Chin Med Assoc* 2021;84:563–76.
26 Heinrich S, Craig AJ, Ma L, *et al*. Understanding tumour cell heterogeneity and its implication for immunotherapy in liver cancer using single-cell analysis. *J Hepatol* 2021;74:700–15.
27 van der Leun AM, Thommen DS, Schumacher TN. $CD8^+$ T cell states in human cancer: insights from single-cell analysis. *Nat Rev Cancer* 2020;20:218–32.
28 Sanmamed MF, Chen L. A Paradigm Shift in Cancer Immunotherapy: From Enhancement to Normalization. *Cell* 2018;175:313–26.
29 Scherl-Mostageer M, Sommergruber W, Abseher R, *et al*. Identification of a novel gene, CDCP1, overexpressed in human colorectal cancer. *Oncogene* 2001;20:4402–8.
30 Urabe F, Kosaka N, Yamamoto Y. Metastatic prostate cancer-derived extracellular vesicles facilitate osteoclastogenesis by transferring the CDCP1 protein. *J Extracell Vesicles* 2023;12:e12312.
31 Alajati A, D'Ambrosio M, Troiani M, *et al*. CDCP1 overexpression drives prostate cancer progression and can be targeted in vivo. *J Clin Invest* 2020;130:2435–50.
32 Wright HJ, Hou J, Xu B, *et al*. CDCP1 drives triple-negative breast cancer metastasis through reduction of lipid-droplet abundance and stimulation of fatty acid oxidation. *Proc Natl Acad Sci U S A* 2017;114:E6556–65.
33 Dagnino S, Bodinier B, Guida F, *et al*. Prospective Identification of Elevated Circulating CDCP1 in Patients Years before Onset of Lung Cancer. *Cancer Res* 2021;81:3738–48.
34 Karachaliou N, Chaib I, Cardona AF, *et al*. Common Co-activation of AXL and CDCP1 in EGFR-mutation-positive Non-Small Cell Lung Cancer Associated With Poor Prognosis. *EBioMedicine* 2018;29:112–27.
35 Harrington BS, He Y, Khan T, *et al*. Anti-CDCP1 immuno-conjugates for detection and inhibition of ovarian cancer. *Theranostics* 2020;10:2095–114.
36 Chopra S, Trepka K, Sakhamuri S, *et al*. Theranostic Targeting of CUB Domain-Containing Protein 1 (CDCP1) in Multiple Subtypes of Bladder Cancer. *Clin Cancer Res* 2023;29:1232–42.
37 Moroz A, Wang Y-H, Sharib JM, *et al*. Theranostic Targeting of CUB Domain Containing Protein 1 (CDCP1) in Pancreatic Cancer. *Clin Cancer Res* 2020;26:3608–15.
38 Khan T, Lyons NJ, Gough M, *et al*. CUB Domain-Containing Protein 1 (CDCP1) is a rational target for the development of imaging tracers and antibody-drug conjugates for cancer detection and therapy. *Theranostics* 2022;12:6915–30.
39 Lim SA, Zhou J, Martinko AJ, *et al*. Targeting a proteolytic neoepitope on CUB domain containing protein 1 (CDCP1) for RAS-driven cancers. *J Clin Invest* 2022;132:e154604.
40 Liu H, Ong S-E, Badu-Nkansah K, *et al*. CUB-domain-containing protein 1 (CDCP1) activates Src to promote melanoma metastasis. *Proc Natl Acad Sci U S A* 2011;108:1379–84.
41 Law ME, Ferreira RB, Davis BJ, *et al*. CUB domain-containing protein 1 and the epidermal growth factor receptor cooperate to induce cell detachment. *Breast Cancer Res* 2016;18:80.
42 Uekita T, Fujii S, Miyazawa Y, *et al*. Oncogenic Ras/ERK signaling activates CDCP1 to promote tumor invasion and metastasis. *Mol Cancer Res* 2014;12:1449–59.
43 Cen Y, Zhu T, Zhang Y, *et al*. hsa_circ_0005358 suppresses cervical cancer metastasis by interacting with PTBP1 protein to destabilize CDCP1 mRNA. *Mol Ther Nucleic Acids* 2022;27:227–40.

44 Huang L, Chen Y, Lai S, *et al*. CUB Domain-Containing Protein -1 Promotes Proliferation, Migration and Invasion in Cervical Cancer Cells. *Cancer Manag Res* 2020;12:3759–69.
45 Jiang P, Gu S, Pan D, *et al*. Signatures of T cell dysfunction and exclusion predict cancer immunotherapy response. *Nat Med* 2018;24:1550–8.
46 Borjini N, Lun Y, Jang G-F, *et al*. CD6 triggers actomyosin cytoskeleton remodeling after binding to its receptor complex. *J Leukoc Biol* 2024;115:450–62.
47 Ogiwara Y, Nakagawa M, Nakatani F. Blocking FSTL1 boosts NK immunity in treatment of osteosarcoma. *Cancer Lett* 2022;537:215690.
48 Wong S-C, Yeh C-C, Zhang X-Y, *et al*. Inhibition of CDCP1 by 8-isopentenylnaringenin synergizes with EGFR inhibitors in lung cancer treatment. *Mol Oncol* 2023;17:1648–65.
49 Cai D, Li J, Liu D, *et al*. Tumor-expressed B7-H3 mediates the inhibition of antitumor T-cell functions in ovarian cancer insensitive to PD-1 blockade therapy. *Cell Mol Immunol* 2020;17:227–36.
50 Wang J, Sun J, Liu LN, *et al*. Siglec-15 as an immune suppressor and potential target for normalization cancer immunotherapy. *Nat Med* 2019;25:656–66.
51 Consuegra-Fernández M, Lin F, Fox DA, *et al*. Clinical and experimental evidence for targeting CD6 in immune-based disorders. *Autoimmun Rev* 2018;17:493–503.
52 Aragón-Serrano L, Carrillo-Serradell L, Planells-Romeo V, *et al*. CD6 and Its Interacting Partners: Newcomers to the Block of Cancer Immunotherapies. *Int J Mol Sci* 2023;24:17510.
53 Enyindah-Asonye G, Li Y, Ruth JH, *et al*. CD318 is a ligand for CD6. *Proc Natl Acad Sci U S A* 2017;114:E6912–21.
54 Xue C, Yao Q, Gu X, *et al*. Evolving cognition of the JAK-STAT signaling pathway: autoimmune disorders and cancer. *Signal Transduct Target Ther* 2023;8:204.
55 Villarino AV, Kanno Y, O'Shea JJ. Mechanisms and consequences of Jak-STAT signaling in the immune system. *Nat Immunol* 2017;18:374–84.
56 Owen KL, Brockwell NK, Parker BS. JAK-STAT Signaling: A Double-Edged Sword of Immune Regulation and Cancer Progression. *Cancers (Basel)* 2019;11:2002.
57 Wee S, Schieven GL, Kirihara JM, *et al*. Tyrosine phosphorylation of CD6 by stimulation of CD3: augmentation by the CD4 and CD2 coreceptors. *J Exp Med* 1993;177:219–23.
58 Velasco-de Andrés M, Casadó-Llombart S, Català C, *et al*. Soluble CD5 and CD6: Lymphocytic Class I Scavenger Receptors as Immunotherapeutic Agents. *Cells* 2020;9:2589.
59 Henriques SN, Oliveira L, Santos RF, *et al*. CD6-mediated inhibition of T cell activation via modulation of Ras. *Cell Commun Signal* 2022;20:184.
60 Gonçalves CM, Henriques SN, Santos RF, *et al*. CD6, a Rheostat-Type Signalosome That Tunes T Cell Activation. *Front Immunol* 2018;9:2994.
61 Chalmers SA, Ayilam Ramachandran R, Garcia SJ, *et al*. The CD6/ALCAM pathway promotes lupus nephritis via T cell–mediated responses. *J Clin Invest* 2022;132:e147334.
62 Chalmers SA, Ayilam Ramachandran R, Garcia SJ, *et al*. The CD6/ALCAM pathway promotes lupus nephritis via T cell-mediated responses. *J Clin Invest* 2022;132:e147334.
63 Castro MAA, Oliveira MI, Nunes RJ, *et al*. Extracellular isoforms of CD6 generated by alternative splicing regulate targeting of CD6 to the immunological synapse. *J Immunol* 2007;178:4351–61.
64 Brunelli E, Minassi A, Appendino G, *et al*. 8-Prenylnaringenin, inhibits estrogen receptor-alpha mediated cell growth and induces apoptosis in MCF-7 breast cancer cells. *J Steroid Biochem Mol Biol* 2007;107:140–8.
65 den Boon JA, Pyeon D, Wang SS, *et al*. Molecular transitions from papillomavirus infection to cervical precancer and cancer: Role of stromal estrogen receptor signaling. *Proc Natl Acad Sci USA* 2015;112:E3255–64.